Hydrogen adsorbed at N-polar InN: Significant changes in the surface electronic properties

A. Eisenhardt, S. Krischok,* and M. Himmerlich

Institut für Physik and Institut für Mikro- und Nanotechnologien, Technische Universität Ilmenau, PF 100565, 98684 Ilmenau, Germany

(Received 13 January 2015; revised manuscript received 20 May 2015; published 12 June 2015)

The interaction of atomic hydrogen and ammonia with as-grown N-polar InN surfaces is investigated using *in situ* photoelectron spectroscopy. Changes in the surface electronic properties, including the band alignment and work function, as well as the chemical bonding states of the substrate and adsorbates are characterized. Ammonia molecules are dissociating at the InN surface, resulting in adsorption of hydrogen species. Consequently, the considerable changes of the chemical and electronic properties of the InN surface during ammonia interaction are almost identical to those found for adsorption of atomic hydrogen. In both cases, hydrogen atoms preferentially bond to surface nitrogen atoms, resulting in the disappearance of the nitrogen dangling-bond-related occupied surface state close to the valence band edge at ∼1.6 eV binding energy and the formation of new occupied electron states at the conduction band edge. Furthermore, a decrease in work function during adsorption from 4.7 to 3.7–3.8 eV, as well as an increase in the surface downward band bending by 0.3 eV, confirm that hydrogen is acting as electron donor at InN surfaces and therefore has to be considered as one main reason for the surface electron accumulation observed at N-polar InN samples exposed to ambient conditions, for example as the dissociation product of molecules. The measured formation and occupation of electronic states above the conduction band minimum occur in conjunction with the observed increase in surface electron concentration and underline the relationship between the energy position of occupied electron states and surface band alignment for InN as a small-band-gap semiconductor.

DOI: 10.1103/PhysRevB.91.245305 PACS number(s): 73.20.At, 73.20.Hb, 81.05.Ea, 82.80.Pv

I. INTRODUCTION

Indium nitride belongs to the class of III-V semiconductor materials with a low band gap [1–3] and electronic properties that provide a great potential for use in electronic and optoelectronic devices [4,5]. However, device realization is still a challenge, especially due to the high intrinsic bulk electron concentration, but also because of the preferred formation of an electron accumulation layer at InN surfaces and its interfaces with other materials [6,7]. During recent years, substantial progress has been made in understanding the reasons that lead to the high surface electron concentrations. Thus, the assumption of electron accumulation being an intrinsic property of all InN surfaces [8] was disproved by *in situ* characterization of as-grown and ultrahigh-vacuum- (UHV-) cleaved polar and nonpolar InN surfaces [9–11]. Furthermore, it was shown that several chemical treatments as well as the interaction of InN surfaces with certain adsorbates [12–21] allow the band bending and the electron density at the surface to be significantly influenced. In this context, experimental studies have shown, in agreement with predictions from density functional theory (DFT) calculations [22–24], that the formation and energetic position of surface states due to surface reconstructions, the formation of In adlayers, and the interaction with adsorbates play important roles [9,25].

Hydrogen is predicted to significantly influence the electronic properties of InN. Theoretical investigations [26,27] as well as experimental results [28–36] reveal that hydrogen is acting as an electron donor in InN, increasing the bulk and surface electron concentrations. In this context, the better quality of InN samples grown by molecular beam epitaxy compared to samples prepared by metal-organic vapor phase epitaxy (MOVPE) was attributed to the higher hydrogen concentration introduced via the NH_3 precursor used in the MOVPE growth process [37]. Density functional theory studies of monatomic hydrogen in InN predict that it can be incorporated either as the interstitial species H_i with two different stable configurations in the InN host matrix (the antibonding or the bond-center configuration) or as substitutional hydrogen on nitrogen sites H_N [27,38]. Interstitial hydrogen species strongly bond to nitrogen while substitutional hydrogen bonds to four indium atoms in a multicenter configuration, acting as a double donor [27,38].

Apart from its impact as a bulk impurity, hydrogen at InN surfaces is rarely studied experimentally. Mainly theoretical work has been performed concerning the stability and lowest-energy surface structures of hydrogen adsorbed at nonpolar and semipolar InN surfaces [39,40] as well as hydrogen species as decomposition products from ammonia dissociated at polar InN surfaces [41–43]. The first experimental studies were published by Bhatta *et al.* [44–46], who investigated N-terminated InN surfaces by high-resolution electron-energy-loss spectroscopy (HREELS) and discussed N-H bonds as possible sources for surface electron accumulation.

In this paper, we present a detailed experimental study of the interaction of hydrogen and ammonia with N-polar InN surfaces using *in situ* photoelectron spectroscopy. We discuss hydrogen-induced modifications of InN surface properties, including the formation of additional electron states above the conduction band minimum, changes in the surface band alignment, the work function, and the formation of surface dipoles.

II. EXPERIMENT

N-polar InN $(000\bar{1})$ films were grown by plasma-assisted molecular beam epitaxy on N-doped C-face SiC$(000\bar{1})$ substrates with a thin GaN buffer layer. After epitaxial growth, the samples were transferred to the analysis chamber without

*stefan.krischok@tu-ilmenau.de

interrupting the ultrahigh-vacuum conditions (base pressure below 2×10^{-10} mbar) and characterized *in situ* by x-ray and UV photoelectron spectroscopy (XPS and UPS). More details about the epitaxial growth and experimental equipment can be found elsewhere [19,47].

To investigate their interaction with adsorbates, the as-grown N-polar InN samples were exposed at room temperature to hydrogen (purity 99.999%, $p_{H_2} = 2.0 \times 10^{-8}$ mbar) or ammonia (purity 99.9999%, $p_{NH_3} = 9.0 \times 10^{-9}$–$1.0 \times 10^{-8}$ mbar) by backfilling the analysis chamber. Prior to each adsorption experiment, the gas supply lines were thoroughly evacuated to a pressure below 1.0×10^{-7} mbar and subsequently filled with 0.5 bar of the respective gas used for the measurement. The molecular hydrogen was additionally activated by a hot filament to obtain atomic hydrogen species. During exposure, the residual gas was monitored by quadrupole mass spectrometry to control the gas purity and ensure the absence of impurities. The pressure was measured with a Bayard-Alpert ionization gauge and used without any further correction to calculate the exposure in langmuirs ($1\ \text{L} = 1.33 \times 10^{-6}$ mbar s). According to these calculations up to 100 L hydrogen and 15 L ammonia were offered. However, one should note that for hydrogen, due to a limited cracking efficiency, the actual amount of atomic species produced is below the calculated total hydrogen exposure. Furthermore, partial activation of NH_3 due to hot filaments of the pressure gauge or the mass spectrometer in the chamber cannot completely be ruled out. Therefore, a comparison between absolute exposure values should be made carefully.

III. RESULTS

Figure 1 shows XPS spectra of the In $3d_{5/2}$ core levels measured during the continuous exposure of the InN surface to hydrogen (left) and ammonia (right). The binding energies of the In $3d_{5/2}$ and N 1*s* (not shown) states after epitaxial growth are 443.8 and 396.2 eV, in agreement with earlier experiments on as-grown N-polar InN samples [19]. Interaction of the InN($000\bar{1}$) surface with hydrogen as well as ammonia leads to

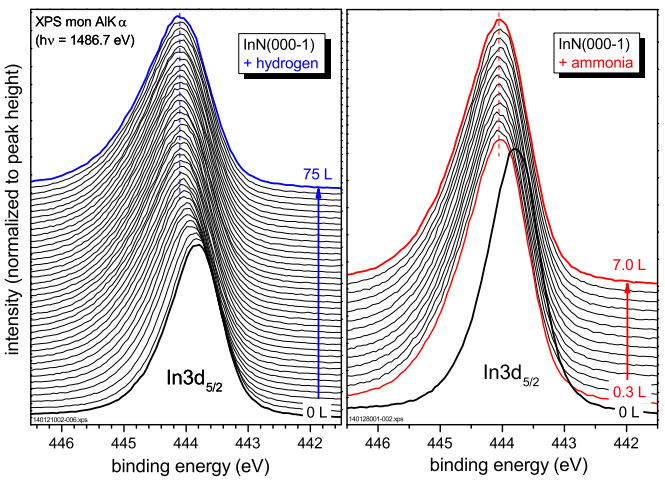

FIG. 1. (Color online) Changes in the XPS In $3d_{5/2}$ core level spectra during hydrogen (left) and ammonia (right) exposure.

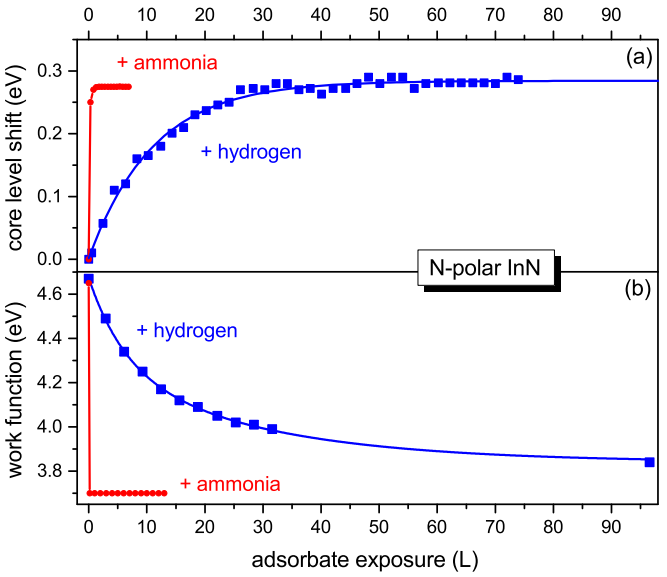

FIG. 2. (Color online) (a) Core level shift ΔV_{bb} to higher binding energy and (b) variation of work function Φ of N-polar InN surfaces as functions of adsorbate exposure for interaction with hydrogen (blue) and ammonia (red).

a shift of the core level binding energies to higher values. In Fig. 2(a), this shift is plotted as a function of exposure for the measurements shown in Fig. 1. In both cases the core levels shift by ~0.3 eV to higher values with increasing exposure, resulting in In $3d_{5/2}$ and N 1*s* binding energies of 444.1 and 396.5 eV, respectively. These values are comparable to those of as-grown In-polar or N-polar InN films that have been subsequently stored in UHV for several days [19]. The valence band maximum (VBM), as determined by linear extrapolation of the trailing edge of the XPS VB spectra, is shifted by the same quantity, starting at about 1.0 eV for as-grown N-polar InN.

Variations in core level and VBM binding energies reflect changes in the surface band bending, which is schematically drawn in Fig. 3. With a band gap of about 0.67 eV and a bulk Fermi level around 0.2 eV above the conduction band minimum (CBM) [48,49], the as-grown N-polar surface exhibits almost flatband conditions with a bend bending (V_{bb}) around ±0.1 eV [9]. Consequently, hydrogen as well as ammonia exposure leads to an increase in the surface downward band bending of $\Delta V_{bb} \sim 0.3$ eV, resulting in a higher surface electron concentration.

Additionally, changes in the work function Φ were measured by UPS (He I), applying a sample bias of −3 V to assure the measurement of the correct onset of secondary electron emission, which was determined by linear extrapolation to zero. The work function of as-grown N-polar InN is typically in the range between 4.6 and 4.7 eV. The change of Φ as a function of hydrogen exposure is plotted in Fig. 2(b). It exhibits a nonlinear monotonic decrease, reaching a value of 3.8 eV at the end of the experiment. The interaction with ammonia also leads to a decrease of Φ to a value in the range between 3.6 and 3.7 eV. However, in accordance with the observed immediate increase in band bending, the work function change is completed after exposure of the first 0.1 L of ammonia. The

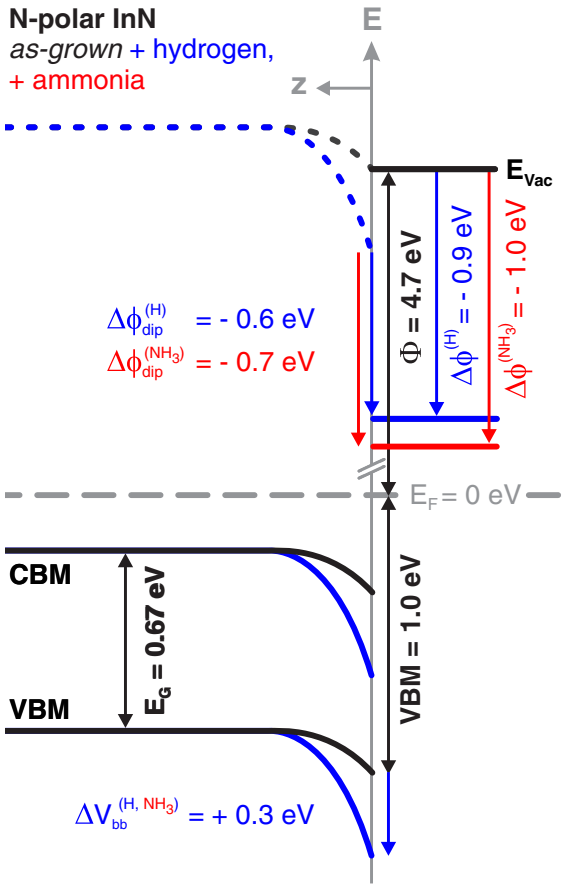

FIG. 3. (Color online) Schematic diagram of the surface band bending V_{bb} for as-grown (black) and adsorbate-covered (blue: hydrogen, red: ammonia) N-polar InN surfaces. Additionally, changes in the work function $\Delta\Phi$ and the resulting values of $\Delta\Phi_{dip}$ due to the effective surface dipole are illustrated.

changes in work function are also depicted in the schematic surface energy diagram in Fig. 3. Based on the experimentally determined values of the changes in band bending ΔV_{bb} and work function $\Delta\Phi$, it is possible to estimate changes in the effective surface dipole at the adsorbate-covered InN surface: $\Delta\Phi_{dip} = \Delta V_{bb} + \Delta\Phi$. For hydrogen $\Delta\Phi_{dip}$ is about -0.6 eV and for ammonia -0.7 eV (see Fig. 3). Hence, in both cases a surface dipole is formed with its positive side pointing away from the sample surface.

To obtain information about the chemical bonding of hydrogen and ammonia with InN(000$\bar{1}$) surfaces, XPS In $3d_{5/2}$ and N 1s spectra, measured before (black) and after (blue or red) adsorbate exposure, are compared in Fig. 4. Additionally, spectra of as-grown In-polar InN (see Ref. [9]) are added in gray. The difference spectra at the right top site are calculated by subtracting the gray spectrum of as-grown In-polar InN from the blue and red spectra of the adsorbate-covered N-polar InN, and fitted with two components at 398.9 and 397.9 eV binding energy.

Besides the peak shift already discussed, a comparison between the shape of XPS spectra of as-grown and adsorbate-covered N-polar InN (Fig. 4) reveals most notably the formation of a pronounced tail at the high-binding-energy side of the

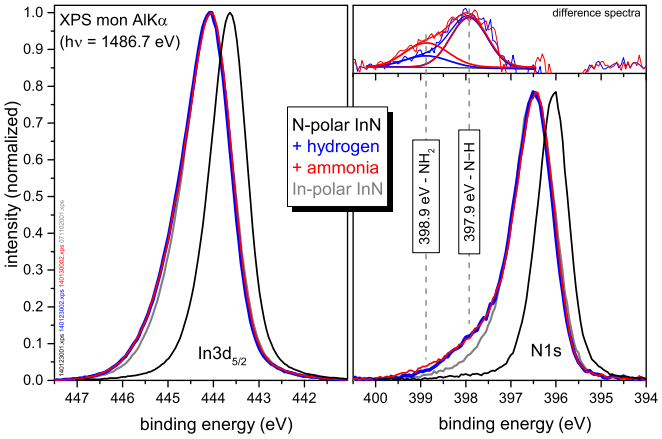

FIG. 4. (Color online) In $3d_{5/2}$ and N 1s core level spectra of as-grown N-polar InN (black), after exposure to 100 L hydrogen (blue) or 15 L ammonia (red). Equivalent spectra of as-grown In-polar InN surfaces from Ref. [9] are added in gray. All spectra are normalized to the same peak height. N 1s difference spectra were calculated by subtracting the spectra of as-grown InN(0001) from the corresponding spectra of adsorbate-covered InN(000$\bar{1}$) surfaces and fitted by two peaks (see upper right corner).

In 3d and N 1s core level spectra after exposure. Taking into account the higher surface electron concentration, an increase in the peak asymmetry due to plasmon losses is expected [50]. Since adsorbate-covered N-polar InN surfaces exhibit a comparable band bending to that of contamination-free as-grown In-polar InN [9], the comparison of the corresponding XPS spectra allows identification of the plasmon-loss-induced contributions to the peak asymmetry. The In 3d core level peak shapes are almost identical, and consequently the observed changes in peak asymmetry are mainly induced by plasmon losses, while the formation of an additional adsorbate-induced chemical bond to surface In atoms is not evident. Comparable results were also found when analyzing the In 4d spectra. The In 4d state measured by UPS using He II radiation is illustrated in Fig. 5. The spectrum of the as-grown sample (black) exhibits the typical In 4d spin-orbit splitting with the maximum of the In $4d_{5/2}$ state at 17.0 eV. Hydrogen adsorption results in a modified In 4d shape, which can be solely explained by the adsorbate-induced changes in surface band bending and electron density as already discussed for the In 3d core level. Consequently, we found – as for the In 3d state – no evidence for additionally formed In-adsorbate chemical states. In contrast, the formation of additional nitrogen bond states at 398.9 and 397.9 eV binding energy can be observed in the N 1s spectra (Fig. 4). Although both surface reactions result in similar chemical adsorbate states, the component at 398.9 eV is higher in intensity for N-polar InN surfaces exposed to ammonia (see the N 1s difference spectra in the top right corner of Fig. 4).

Furthermore, adsorbate-induced changes in the UPS and XPS valence band spectra were investigated (see Fig. 5). Since the changes are almost identical for hydrogen and ammonia exposure, only the spectra for hydrogen exposure are shown in Fig. 5. The XPS VB spectrum of as-grown N-polar InN is characterized by two main structures at ~2.5 and 6.2 eV

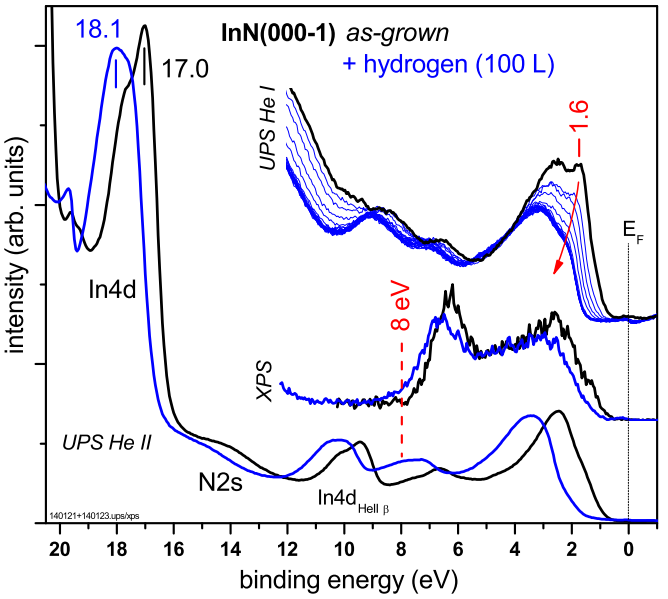

FIG. 5. (Color online) Valence band spectra of N-polar InN surfaces measured using He II (bottom), monochromated Al $K\alpha$ (center) and He I (top) radiation before (black) as well as during and after hydrogen exposure (blue).

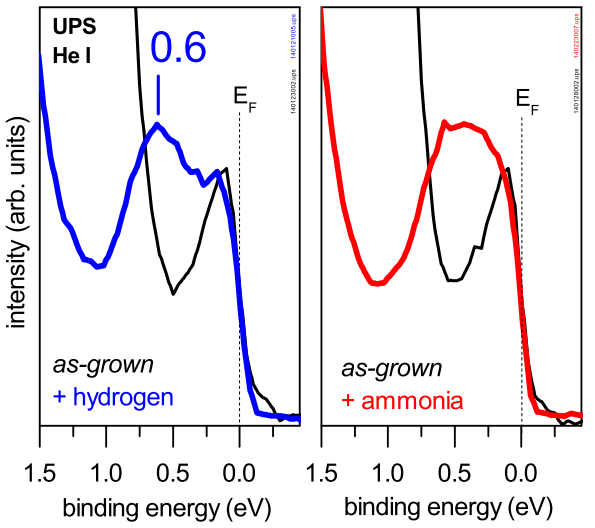

FIG. 6. (Color online) UPS He I spectra of N-polar InN showing the electron emission above the valence band maximum. Interaction with hydrogen (blue) or ammonia leads to the formation of additional electron states in the region between zero and 1.0 eV binding energy. Spectral contributions from satellite lines (He $I_{\beta,\gamma}$) were removed in this figure by subtraction of their relative intensities.

with a higher intensity of the latter [9]. Hydrogen as well as ammonia exposure leads to a change in the intensity ratio between these two structures. Pronounced new hydrogen-induced components cannot be identified in the XPS VB region, although one might speculate about a slight intensity increase around 8 eV. Such a weak intensity increase also occurs in the He II VB spectrum (lower region of Fig. 5), while the UPS He I spectra (upper region of Fig. 5) do not show any additional adsorbate-induced VB component in this energy region. The He I measurements clearly demonstrate the saturation of the nitrogen dangling-bond-induced surface state at 1.6 eV [9] induced by the adsorption of hydrogen. The high reactivity of this surface state was already observed during the interaction of N-polar InN with oxygen [19].

An obvious change in the electronic structure can be observed at the Fermi edge E_F (see the enlarged He I spectra in Fig. 6) after exposure to hydrogen (left) or ammonia (right). After growth (black lines), an emission at the Fermi level is observed due to the degeneracy of InN and the existence of occupied bulk states in the CB. Interaction with hydrogen or ammonia results in additional occupied electron states in the region between zero and 1.0 eV binding energy.

Comparable adsorption experiments as for hydrogen and ammonia were also performed using ethane (purity 99.95%, $p_{C_2H_6} = 1.0 \times 10^{-9}$–$1.0 \times 10^{-8}$ mbar, exposure 100 L) as another hydrogen-containing molecule. The analyses of ethane interaction revealed no significant changes in the chemical and electronic properties of the substrate: no formation of carbon- or hydrogen-related components in the XPS or UPS spectra was found, the band bending did not increase, and the surface state emission at the VBM did not disappear. Besides documenting the low reactivity of ethane, these measurements prove that the observed changes during hydrogen and ammonia interaction are not affected by side reactions due to reactive molecules from the residual gas in the UHV chamber or contaminations in the gas inlet used.

IV. DISCUSSION

The experimental results demonstrate a strong modification of the surface electronic properties of N-polar InN due to the interaction with hydrogen and ammonia. As has been already demonstrated in former studies, as-grown N-polar InN surfaces exhibit a reduced downward band bending in comparison to as-grown In-polar InN films or samples that have been stored under ambient conditions due to differences in the surface structure and the energetic position of surface electronic states [9,19]. Typically the VBM lies 0.8–1.0 eV below the Fermi level. Exposure to hydrogen or ammonia leads to an increase in energy distance between the surface Fermi level and VBM by 0.3 eV (see Fig. 3). In parallel, the core level binding energies and the peak asymmetry, related to surface plasmon losses [50], increase. These changes can be explained by an increase in the surface downward band bending, as illustrated in Fig. 3, tantamount to an increase in surface electron concentration. Additionally, a decrease in the work function was measured during the adsorption experiments, leading to an additional potential of -0.6 to -0.7 eV caused by an effective surface dipole. Consequently, the adsorbed species, which are bound to the topmost surface atoms, partially transfer electron charge to the InN surface (which increases the InN surface electron density) and form a surface dipole with its positive side pointing away from the surface. From theoretical investigations [26,27] as well as experimental results [28–36], it is known that hydrogen acts as electron donor in InN, increasing the bulk and surface electron concentrations. Our investigations, especially the interaction experiments with pure hydrogen, endorse and underline these results.

The magnitude of the band bending and the electron concentration profile at the surface are directly linked to each other and depend on the bulk electron concentration of the InN film as well as the surface sheet carrier density, which is connected with the density of surface states. These values can be calculated by solving the Schrödinger and Poisson equations self-consistently using numerical approaches [17,51,52]. Typically, the density of surface states is in the range of 10^{13} cm^{-2} for samples that exhibit strong surface electron accumulation as found for InN films with different surface orientations and varying bulk electron concentrations [8,13]. In the case of the prepared N-polar InN samples, the bulk electron concentration is $\sim 1\times 10^{19}$ cm^{-3}, comparable to that in In-polar samples with strong electron accumulation [47], prepared using the same experimental setup. Consequently, the Fermi level in the bulk for both types of polarity is ~0.2 eV above the CBM [48,49]. However, as-grown N-polar samples exhibit almost flatband conditions as we find a very low value of bend bending (V_{bb}) around ±0.1 eV [9]. After hydrogen adsorption, the observed shift of occupied electron states away from the Fermi level is induced by a downward bending of the bands at the surface ($\Delta V_{bb} \sim 0.3$ eV – see Fig. 3), and the surface band alignment is then comparable to that of the as-grown In-polar InN samples [47]. This effect can also be interpreted in terms of the Poisson equation: hydrogen adsorption increases the density of electron states N_{ss} at the N-polar InN surface. These localized surface states induce a reaction of the electrons in the interface region and the bulk, leading to a modification of the surface electron distribution by charge transfer. Since the resulting value of band bending is directly dependent on N_{ss}, the amount of adsorbed hydrogen directly influences the surface electron accumulation layer for N-polar InN. As a rough estimate, based on a comparison with the dependency $V_{bb}(N_{ss})$ for a bulk electron concentration of 10^{18} cm^{-3} given in Fig. 3 of Ref. [17], we conclude that the density of surface states generated due to hydrogen adsorption is in the mid-10^{12} cm^{-2} range.

Comparing the surface electronic structure of N-polar InN after hydrogen and ammonia adsorption, no pronounced differences are found – both experiments result in comparable changes in the occupied surface states close to the Fermi edge, the surface band bending, and the work function. Therefore we conclude that during ammonia interaction, hydrogen atoms are split off the dissociating ammonia molecules and attach to the dangling bonds of the InN surface. This result is in good agreement with theoretical results from Walkosz *et al.*, who investigated the reaction pathway of NH_3 at In-polar InN(0001) surfaces [41], discussing the possible decomposition of ammonia as well as stable adsorption sites for the decomposition products (NH_3, NH_2, NH, N, and H). They found that the NH_3 adsorption energy is comparable to the barrier for the first decomposition reaction. Hence, ammonia decomposition and desorption are competitive processes, while the decomposition and the adsorption of the thermodynamically more stable $NH_2 + H$ configuration dominates at appropriate ammonia pressure. Furthermore, they found that the subsequent decomposition steps mainly take place by H transfer, resulting in a complete dissociation of ammonia with N and H species at the surface. Single N atoms can easily pair up after surface diffusion and can desorb as molecular N_2 afterwards. In contrast, adsorbed hydrogen species preferentially remain at the surface due to a high activation barrier for H_2 formation [41].

Concerning the identification of hydrogen adsorption sites at N-polar InN surfaces, a comparison of the presented XPS and UPS results with available literature gives valuable indications. For instance, it is known that NH_x ($x \leqslant 3$) components in the N 1*s* spectrum of InN are expected at binding energies in the range between 397.7 and 400.4 eV [14,21,53–56]. Furthermore, results from HREELS measurements at N-terminated InN surfaces [44,45,57] as well as calculations concerning the stability of hydrogen at polar and nonpolar surfaces [39] confirm the preferred formation of N-H bonds at InN surfaces. Walkosz *et al.* found that the lowest-energy structure of polar InN exposed to ammonia consists of NH_2 species [42], and Suzuki *et al.* theoretically analyzed the surface structures of polar InN surfaces in the presence of hydrogen and NH_x ($1 \leqslant x \leqslant 3$) [40,43] and found that for N-polar InN, the stable surface shows a geometry with N-H bonds between the H adatoms and N surface atoms. Furthermore, Janotti and Van de Walle investigated the effects of monatomic hydrogen in bulk InN [27] by DFT and found that hydrogen is most stable at interstitial sites (H_i), forming strong bonds to the nitrogen atoms in conjunction with a weakening and cracking of In-N bonds. Therefore, we assign the additional components in the N 1*s* spectra (Fig. 4) to hydrogen-induced bonds, whereby the component at 397.9 eV binding energy corresponds to N-H and the one at 398.9 eV is characteristic for NH_2. In this context, the slight difference in the peak intensity of the component at 398.9 eV after hydrogen and ammonia exposure is most likely caused by a higher amount of hydrogen at the ammonia-exposed surface.

Besides hydrogen bound to nitrogen, Janotti and Van de Walle furthermore described hydrogen in InN substituting for nitrogen atoms and binding to the In atoms in a multicenter bond configuration (H_N) [27], which is very stable, has a low formation energy, and acts as a double donor ($H_N{}^{2+}$). It is worth mentioning that in this configuration the formation of a bonding state 6.5 eV below the VBM and an antibonding state 6 eV above the CBM was predicted [38,58]. Although the surface configuration is expected to be different from that of the bulk, a corresponding state at the surface might explain the weak structure at about 8 eV below E_F in the VB spectra in Fig. 5. However, as already discussed, we found no indications for the formation of In-H bonds and no change in the In:N ratio in the photoemission experiments. Therefore, we tend to exclude a significant amount of hydrogen substituting for nitrogen. Consequently, the changes in the VB spectra at about 8 eV are more likely caused by structural relaxation or charge redistribution of the InN top surface layers caused by the hydrogen adsorbates in general. The observation of comparable effects during the adsorption of potassium at InN(0001) surfaces [59] further supports this picture. Additionally, the effect of H-induced relaxation of the surface atom arrangement combined with local electron transfer processes might also explain the observed changes in the intensity ratio of the two main features around 2.5 and 6.2 eV in the XPS valence band spectra.

While hydrogen-induced components could not clearly be identified in the VB region, significant changes are observed

around the CBM. Figure 6 illustrates the formation of occupied electron states between E_F and ∼1.0 eV below E_F, with a peak at 0.6 eV after hydrogen adsorption. This signal could be an indication of the formation of a surface state in this energy range. However, due to a lack of theoretical investigations, the assignment of this state to any surface-adsorbate configuration is rather difficult. A surface state at about 0.7 eV was already observed at as-grown In-polar InN surfaces [9] and theoretical investigations assigned it to occupied bonds of In adatoms [22–24]. Furthermore, according to Refs. [27,60,61], adjacent indium atoms in defect configurations with reduced bonding distance or irregular In-In bonds as well as nitrogen vacancies would create comparable electronic states in the gap and above the CBM. However, in our case the formation of In-In bonds and In adlayers can be ruled out since a constant In:N ratio was measured during the experiments presented here and no indication of surface indium accumulation was found in the XPS and UPS spectra [47]. The origin of this feature could further be speculated to be the existence of defect states such as nitrogen vacancies induced by hydrogen adsorption. For reasons already discussed above, this appears to be no suitable explanation, and defects do not significantly contribute to the observed electronic state, since the corresponding states would be detected for the as-grown N-polar InN surfaces. Therefore we conclude that the peak at 0.6 eV is most likely a hydrogen-induced surface state.

Furthermore it should be mentioned that the observed increase in electron emission in the CB region and the downward bending of the bands could also be an effect of occupation of InN CB states at the surface, mediated via relaxation of electrons from hydrogen-induced adsorbate states located high in the CB. With photoluminescence the energy level of bulk H donors in hydrogenated InN samples was determined to be about 10 meV below the conduction band edge [31]. This would correspond to a binding energy ∼0.6–0.7 eV below E_F and could therefore explain the detected surface state in our spectra. Independent of the exact details of the surface configuration and the exact energy alignment of the corresponding states, which are in particular due to the lack of theoretical calculations for hydrogen adsorbates at the N-polar InN surface beyond the scope of this investigation, the hydrogen-induced changes of electron states around the Fermi edge in our experiments are results of the combination of occupation of conduction band states by charge transfer processes from energetically higher electron levels of the hydrogen adsorbate (electron donation) and the formation of well-defined surface states that develop during the hydrogen adsorption process, including the saturation of nitrogen dangling bonds of additional (In)N-H surface-adsorbate configurations. These effects are strongly interconnected to each other and cannot therefore be considered independently.

The occupation of the empty CB states and the formation of electron states close to and above the CBM lead to a shift of the energy position of the surface Fermi level, or in other words a downward bending of the valence and conduction bands, which is reflected in the observed changes in core and valence electron binding energy. Consequently, once more the strong relation between the energetic positions of occupied electron states and surface band alignment, as already described for as-grown as well as oxygen- or potassium-covered polar and nonpolar InN surfaces [9,59], is manifested.

V. CONCLUSION

The interaction of hydrogen and ammonia with N-polar InN surfaces was investigated using *in situ* photoelectron spectroscopy. This study reveals experimentally that hydrogen atoms preferentially attach to the free bonds of the nitrogen surface atoms, leading to the disappearance of the nitrogen dangling-bond-related surface state at the valence band edge. The ammonia molecules dissociate at the N-polar InN surface, leading to adsorbed hydrogen species comparable to those observed during the interaction with atomic hydrogen. The modification of surfaces states and the related processes strongly affect the electron concentration and surface band bending of N-polar InN. A broadening of the electron emission region above the CBM was detected which is caused by the formation and occupation of additional electron states. It results in a shift of the position of the surface Fermi level which correlates with the simultaneously observed increase in the surface downward band bending by ∼0.3 eV at the adsorbate covered N-polar InN surface. Together with the measured decrease in work function, one can conclude that hydrogen adsorbed at N-polar InN surfaces partially transfers its electron charge to the substrate, resulting in an increase in the surface electron concentration of the semiconductor. Therefore, hydrogen as dissociation product of many different ambient molecules has to be considered as one main reason for the strong electron accumulation typically observed at N-polar surfaces. Based on the performed study, the nature of hydrogen acting as electron supplier at InN surfaces is demonstrated and the related changes in electronic structure support the theory that hydrogen acts as electron donor in the III-N semiconductor InN.

ACKNOWLEDGMENT

Financial support by the DFG under Grant No. SCHA 435/25 and by the Carl-Zeiss-Stiftung is gratefully acknowledged.

[1] V. Yu. Davydov, A. A. Klochikhin, R. P. Seisyan, V. V. Emtsev, S. V. Ivanov, F. Bechstedt, J. Furthmüller, H. Harima, A. V. Mudryi, J. Aderhold, O. Semchinova, and J. Graul, Phys. Status Solidi B **229**, R1 (2002).

[2] W. Walukiewicz, J. W. Ager, K. M. Yu, Z. Liliental-Weber, J. Wu, S. X. Li, R. E. Jones, and J. D. Denlinger, J. Phys. D **39**, R83 (2006).

[3] P. Schley, R. Goldhahn, G. Gobsch, M. Feneberg, K. Thonke, X. Wang, and A. Yoshikawa, Phys. Status Solidi B **246**, 1177 (2009).

[4] V. M. Polyakov and F. Schwierz, Appl. Phys. Lett. **88**, 032101 (2006).

[5] T. D. Veal, C. F. McConville, and W. J. Schaff, *Indium Nitride and Related Alloys* (CRC Press, Boca Raton, FL, 2010).

[6] I. Mahboob, T. D. Veal, C. F. McConville, H. Lu, and W. J. Schaff, Phys. Rev. Lett. **92**, 036804 (2004).

[7] H. Lu, W. J. Schaff, L. F. Eastman, and C. E. Stutz, Appl. Phys. Lett. **82**, 1736 (2003).

[8] P. D. C. King, T. D. Veal, C. F. McConville, F. Fuchs, J. Furthmüller, F. Bechstedt, P. Schley, R. Goldhahn, J. Schörmann, D. J. As, K. Lischka, D. Muto, H. Naoi, Y. Nanishi, H. Lu, and W. J. Schaff, Appl. Phys. Lett. **91**, 092101 (2007).

[9] A. Eisenhardt, S. Krischok, and M. Himmerlich, Appl. Phys. Lett. **102**, 231602 (2013).

[10] C. L. Wu, H. M. Lee, C. T. Kuo, C. H. Chen, and S. Gwo, Phys. Rev. Lett. **101**, 106803 (2008).

[11] P. Ebert, S. Schaafhausen, A. Lenz, A. Sabitova, L. Ivanova, M. Dahne, Y. L. Hong, S. Gwo, and H. Eisele, Appl. Phys. Lett. **98**, 062103 (2011).

[12] C. T. Kuo, S. C. Lin, K. K. Chang, H. W. Shiu, L. Y. Chang, C. H. Chen, S. J. Tang, and S. Gwo, Appl. Phys. Lett. **98**, 052101 (2011).

[13] W. M. Linhart, T. D. Veal, P. D. C. King, G. Koblmüller, C. S. Gallinat, J. S. Speck, and C. F. McConville, Appl. Phys. Lett. **97**, 112103 (2010).

[14] Y. H. Chang, Y. S. Lu, Y. L. Hong, C. T. Kuo, S. Gwo, and J. A. Yeh, J. Appl. Phys. **107**, 043710 (2010).

[15] L. R. Bailey, T. D. Veal, C. E. Kendrick, S. M. Durbin, and C. F. McConville, Appl. Phys. Lett. **95**, 192111 (2009).

[16] V. Lebedev, C. Y. Wang, V. Cimalla, S. Hauguth, T. Kups, M. Ali, G. Ecke, M. Himmerlich, S. Krischok, J. A. Schaefer, O. Ambacher, V. M. Polyakov, and F. Schwierz, J. Appl. Phys. **101**, 123705 (2007).

[17] V. Cimalla, V. Lebedev, C. Y. Wang, M. Ali, G. Ecke, V. M. Polyakov, F. Schwierz, O. Ambacher, H. Lu, and W. J. Schaff, Appl. Phys. Lett. **90**, 152106 (2007).

[18] A. Eisenhardt, S. Reiß, M. Himmerlich, J. A. Schaefer, and S. Krischok, Phys. Status Solidi A **207**, 1037 (2010).

[19] A. Eisenhardt, M. Himmerlich, and S. Krischok, Phys. Status Solidi A **209**, 45 (2012).

[20] S. Reiß, A. Eisenhardt, S. Krischok, and M. Himmerlich, Phys. Status Solidi C **11**, 428 (2014).

[21] T. Nagata, G. Koblmüller, O. Bierwagen, C. S. Gallinat, and J. S. Speck, Appl. Phys. Lett. **95**, 132104 (2009).

[22] D. Segev and C. G. Van de Walle, Europhys. Lett. **76**, 305 (2006).

[23] C. G. Van de Walle and D. Segev, J. Appl. Phys. **101**, 081704 (2007).

[24] A. Belabbes, J. Furthmüller, and F. Bechstedt, Phys. Rev. B **84**, 205304 (2011).

[25] W. M. Linhart, J. Chai, R. J. H. Morris, M. G. Dowsett, C. F. McConville, S. M. Durbin, and T. D. Veal, Phys. Rev. Lett. **109**, 247605 (2012).

[26] S. Limpijumnong and C. G. Van De Walle, Phys. Status Solidi B **228**, 303 (2001).

[27] A. Janotti and C. G. Van de Walle, Appl. Phys. Lett. **92**, 032104 (2008).

[28] D. C. Look, H. Lu, W. J. Schaff, J. Jasinski, and Z. Liliental-Weber, Appl. Phys. Lett. **80**, 258 (2002).

[29] E. A. Davis, S. F. J. Cox, R. L. Lichti, and C. G. Van de Walle, Appl. Phys. Lett. **82**, 592 (2003).

[30] C. S. Gallinat, G. Koblmüller, J. S. Brown, S. Bernardis, J. S. Speck, G. D. Chern, E. D. Readinger, H. G. Shen, and M. Wraback, Appl. Phys. Lett. **89**, 032109 (2006).

[31] G. Pettinari, F. Masia, M. Capizzi, A. Polimeni, M. Losurdo, G. Bruno, T. H. Kim, S. Choi, A. Brown, V. Lebedev, V. Cimalla, and O. Ambacher, Phys. Rev. B **77**, 125207 (2008).

[32] V. Darakchieva, N. P. Barradas, M. Y. Xie, K. Lorenz, E. Alves, M. Schubert, P. O. A. Persson, F. Giuliani, F. Munnik, C. L. Hsiao, L. W. Tu, and W. J. Schaff, Physica B **404**, 4476 (2009).

[33] S. Ruffenach, M. Moret, O. Briot, and B. Gil, Appl. Phys. Lett. **95**, 042102 (2009).

[34] C. S. Gallinat, G. Koblmüller, and J. S. Speck, Appl. Phys. Lett. **95**, 022103 (2009).

[35] V. Darakchieva, K. Lorenz, N. P. Barradas, E. Alves, B. Monemar, M. Schubert, N. Franco, C. L. Hsiao, L. C. Chen, W. J. Schaff, L. W. Tu, T. Yamaguchi, and Y. Nanishi, Appl. Phys. Lett. **96**, 081907 (2010).

[36] V. Darakchieva, M. Y. Xie, D. Rogalla, H. W. Becker, K. Lorenz, E. Alves, S. Ruffenach, M. Moret, and O. Briot, Phys. Status Solidi A **208**, 1179 (2011).

[37] S. Ruffenach, M. Moret, O. Briot, and B. Gil, Phys. Status Solidi A **207**, 9 (2010).

[38] C. G. Van de Walle, J. L. Lyons, and A. Janotti, Phys. Status Solidi A **207**, 1024 (2010).

[39] T. Akiyama, T. Yamashita, K. Nakamura, and T. Ito, J. Cryst. Growth **318**, 79 (2011).

[40] H. Suzuki, R. Togashi, H. Murakami, Y. Kumagai, and A. Koukitu, Jpn. J. Appl. Phys. **46**, 5112 (2007).

[41] W. Walkosz, P. Zapol, and G. B. Stephenson, J. Chem. Phys. **137**, 054708 (2012).

[42] W. Walkosz, P. Zapol, and G. B. Stephenson, Phys. Rev. B **85**, 033308 (2012).

[43] H. Suzuki, R. Togashi, H. Murakami, Y. Kumagai, and A. Koukitu, Phys. Status Solidi C **8**, 2267 (2011).

[44] R. P. Bhatta, B. D. Thoms, M. Alevli, V. Woods, and N. Dietz, Appl. Phys. Lett. **88**, 122112 (2006).

[45] R. P. Bhatta, B. D. Thoms, M. Alevli, and N. Dietz, Surf. Sci. **601**, L120 (2007).

[46] R. P. Bhatta, B. D. Thoms, M. Alevli, and N. Dietz, Surf. Sci. **602**, 1428 (2008).

[47] M. Himmerlich, A. Eisenhardt, J. A. Schaefer, and S. Krischok, Phys. Status Solidi B **246**, 1173 (2009).

[48] P. Schley, R. Goldhahn, A. T. Winzer, G. Gobsch, V. Cimalla, O. Ambacher, H. Lu, W. J. Schaff, M. Kurouchi, Y. Nanishi, M. Rakel, C. Cobet, and N. Esser, Phys. Rev. B **75**, 205204 (2007).

[49] K. Kloeckner, M. Himmerlich, R. J. Koch, V. M. Polyakov, A. Eisenhardt, T. Haensel, S. I.-U. Ahmed, S. Krischok, and J. A. Schaefer, Phys. Status Solidi C **7**, 173 (2010).

[50] P. D. C. King, T. D. Veal, H. Lu, S. A. Hatfield, W. J. Schaff, and C. F. McConville, Surf. Sci. **602**, 871 (2008).

[51] T. D. Veal, L. F. J. Piper, W. J. Schaff, and C. F. McConville, J. Cryst. Growth **288**, 268 (2006).

[52] P. D. C. King, T. D. Veal, and C. F. McConville, Phys. Rev. B **77**, 125305 (2008).

[53] Y. Bu, L. Ma, and M. C. Lin, J. Vac. Sci. Technol. A **11**, 2931 (1993).

[54] C. F. Chen, C. L. Wu, and S. Gwo, Appl. Phys. Lett. **89**, 252109 (2006).

[55] M. Krawczyk, A. Biliniski, J. W. Sobczak, S. Ben Khallfa, C. Robert-Gournet, L. Bideux, B. Gruzza, and G. Monier, Surf. Sci. **601**, 3722 (2007).

[56] K. S. A. Butcher, A. J. Fernandes, P. P. T. Chen, M. Wintrebert-Fouquet, H. Timmers, S. K. Shrestha, H. Hirshy, R. M. Perks, and B. F. Usher, J. Appl. Phys. **101**, 123702 (2007).

[57] A. Acharya, B. Thoms, N. Nepal, and J. Eddy, C.R., J. Vac. Sci. Technol. A **33**, 021401 (2015).

[58] A. Janotti, J. L. Lyons, and C. G. Van de Walle, Phys. Status Solidi A **209**, 65 (2012).

[59] A. Eisenhardt, S. Reiß, S. Krischok, and M. Himmerlich, J. Appl. Phys. **115**, 043716 (2014).

[60] E. Kalesaki, J. Kioseoglou, L. Lymperakis, P. Komninou, and T. Karakostas, Appl. Phys. Lett. **98**, 072103 (2011).

[61] C. Stampfl, C. G. Van de Walle, D. Vogel, P. Krüger, and J. Pollmann, Phys. Rev. B **61**, R7846 (2000).